

PAPER • OPEN ACCESS

# Assessment of optical, mechanical and nonlinear properties of potassium acid phthalate single crystal: a potential candidate for optoelectronic applications

Recent citations

- [Growth and Characterization of Single Crystals of L-Histidine Hydrochloride Monohydrate for Nonlinear Optical Applications](#)  
Sudha Yadav *et al*

To cite this article: Manju Kumari *et al* 2020 *Mater. Res. Express* 7 015705

View the [article online](#) for updates and enhancements.

 <p>The Electrochemical Society Advancing solid state &amp; electrochemical science &amp; technology 2021 Virtual Education</p> <p><b>Fundamentals of Electrochemistry:</b> Basic Theory and Kinetic Methods Instructed by: <b>Dr. James Noël</b> Sun, Sept 19 &amp; Mon, Sept 20 at 12h–15h ET</p> <p>Register early and save!</p>	
--	--

# Materials Research Express



## PAPER

# Assessment of optical, mechanical and nonlinear properties of potassium acid phthalate single crystal: a potential candidate for optoelectronic applications

### OPEN ACCESS

RECEIVED  
8 November 2019

REVISED  
27 November 2019

ACCEPTED FOR PUBLICATION  
13 December 2019

PUBLISHED  
13 January 2020

Original content from this work may be used under the terms of the [Creative Commons Attribution 4.0 licence](#).

Any further distribution of this work must maintain attribution to the author(s) and the title of the work, journal citation and DOI.



Manju Kumari<sup>1,2</sup>, N Vijayan<sup>2,3</sup> , Debabrata Nayak<sup>1,2</sup>, Mahesh Kumar<sup>2</sup>, Govind Gupta<sup>1,2</sup>  and R P Pant<sup>2</sup>

<sup>1</sup> Academy of Scientific and Innovative Research, CSIR-National Physical Laboratory, New Delhi –110012, India

<sup>2</sup> CSIR-National Physical Laboratory, Dr K S Krishnan Road, New Delhi—110 012, India

<sup>3</sup> Author to whom any correspondence should be addressed.

E-mail: [nvijayan@nplindia.org](mailto:nvijayan@nplindia.org) and [vnjphy@gmail.com](mailto:vnjphy@gmail.com)

**Keywords:** single crystal, nonlinear optical (NLO) materials, semi-organic, time resolved PL, mechanical properties, X-ray diffraction

## Abstract

A good optical quality semi-organic single crystal of Potassium Acid Phthalate (KAP) was harvested from aqueous solution by using slow evaporation solution growth technique (SEST) at ambient condition. The defect free single crystal of KAP was analyzed by different instrumentation techniques, for checking its compatibility for different applications. Its unit cell dimensions and phase purity was examined by powder X-ray diffraction (PXRD) and found that it crystallizes in orthorhombic with non-centrosymmetric in nature. The quality of the grown ingot was assessed by high resolution X-ray diffraction (HRXRD) technique and found that, the crystalline quality is better with less grain boundaries. Its optical properties were scrutinized by UV–vis., photoluminescence (PL) and time resolved photoluminescence (TRPL) measurements respectively. The mechanical stability of the grown crystal was tested by Vickers microhardness method and found that the grown crystal shows indentation size effect (ISE) which was explained using different theoretical models. Its third order nonlinear optical properties were studied by Z-scan measurement by using Ti:Sapphire laser as a source and determined its nonlinear absorption coefficient ( $\beta$ ) and it was found that the KAP crystal is one of the preferable choices for optical limiting applications.

## 1. Introduction

The enormous improvements in the current technology require potential nonlinear optical materials which is useful in the area of opto-electronics, optical computing, photonics, colour display etc [1, 2]. The title compound of KAP is one of the such potential materials having molecular formula ( $K(C_6H_4COOH.COO)$ ). It is also used as a crystal analyzer for long-wave X-ray spectrometers, highly oriented film of conjugated polymers [3–6]. It also exhibits pyroelectric, piezoelectric, elastic properties which is useful in variety of applications [7–9]. KAP is a semi-organic single crystal in alkali acid phthalate family having orthorhombic symmetry with the space group of  $Pca2_1$ . Acid phthalate ion chains and potassium ions are contained in the ionic configuration of potassium acid phthalate. The structure consists of short O–H–O hydrogen bonds through the ‘a’ glide which is at right angle to b axis. The detailed structural analysis was already reported by Okaya *et al* [10]. The defect free single crystals of KAP were used as harmonic generators in the area of laser applications. Even though, many methods are available for the growth of KAP single crystals [11–14], we have adopted inexpensive SEST for the growth of bulk size single crystal of the title compound. In the current experimental study, we focus on the growth and different characterization analyses which are very important for making any suitable optical devices.

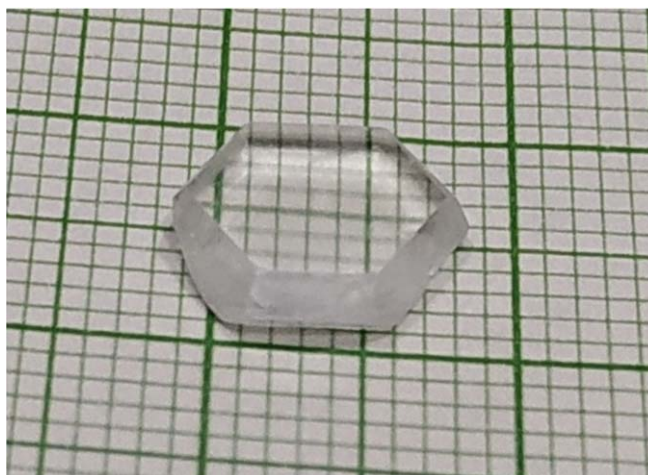


Figure 1. Photograph of grown KAP single crystal.

## 2. Experimental

### 2.1. Crystal growth

The commercially available KAP salt with high purity was taken as the raw material and its purity was enhanced by successive recrystallization processes using deionized water as the solvent. To get good and high optical quality crystal, the most essential feature is purification of material and it is necessary to increase purity up to a best level to use the crystal in different applications. The recrystallization processes is helping to remove the unwanted impurities in the existing raw material and indirectly helps for making quality optical devices. The purified salt of KAP was used to prepare the solution and the solubility was evaluated using the expression given below [9]:-

$$C(T) = 9.283 - 0.059T + 0.0058T^2 \quad (1)$$

where  $C(T)$  represents the equilibrium concentration at a function of temperature  $T$  ( $^{\circ}\text{C}$ ). A saturated solution was prepared with the help of a magnetic stirrer and filtered using Whatman filter paper. After that it was covered with a perforated plastic cover and the whole setup was kept in the constant temperature bath (CTB) at  $40^{\circ}\text{C}$ . After a time period of 25 days, good quality single crystals were found from the mother liquor with the dimensions of  $10\text{ mm} \times 9\text{ mm} \times 2\text{ mm}$  and it is represented in figure 1.

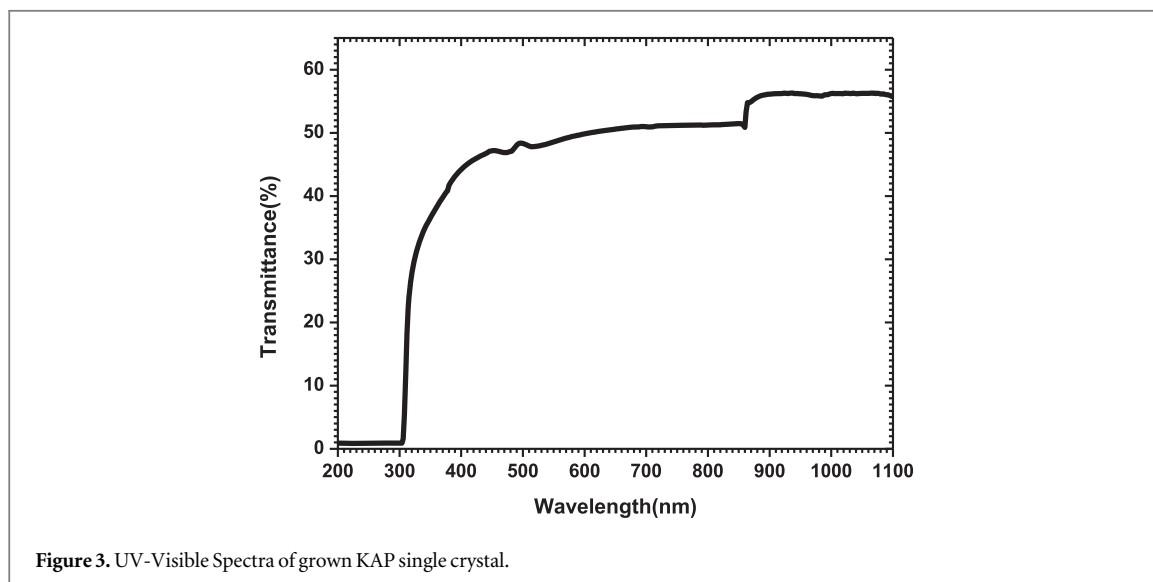
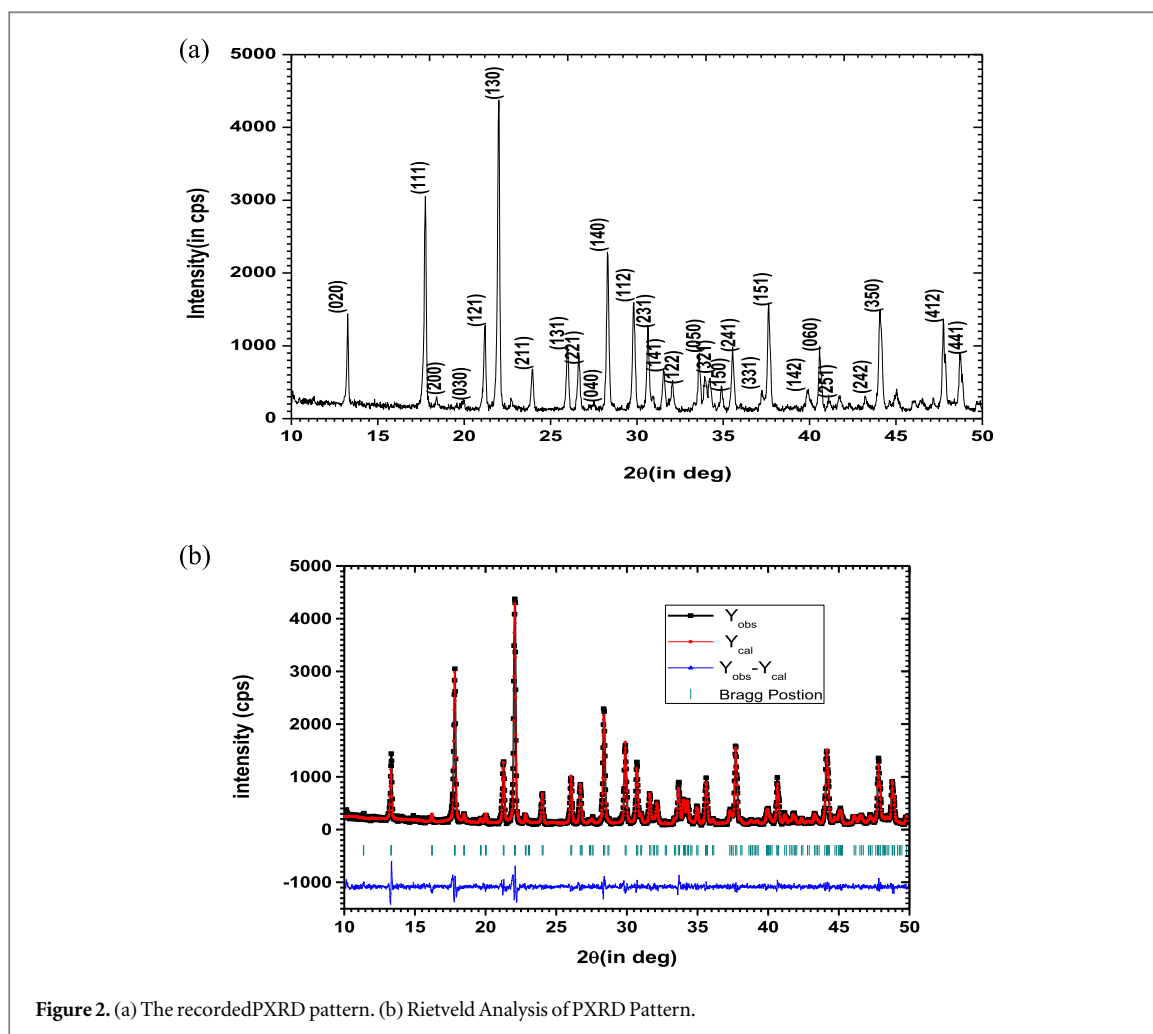
## 3. Results and discussion

### 3.1. Powder X-ray diffraction

In order to know the lattice dimensions of the title compound, the grown crystals were crushed into powder with identical crystallite size. Then the fine powder was subjected to powder X-ray diffraction (PXRD) by using Rigaku (Ultima-IV) X-ray diffractometer which is equipped with Cu X-ray source (Wavelength ( $\lambda$ ) =  $1.541836\text{ \AA}$ ). The measurement was carried out with the  $2\theta$  positions ranging from  $10^{\circ}$  to  $50^{\circ}$  at a scanning rate of  $0.05^{\circ}\text{ s}^{-1}$ . The recorded PXRD pattern is represented in figure 2(a). The experimental peaks were indexed and having good coincidence with the reported literature [15]. The lattice parameters were calculated using Rietveld analysis and found that  $a = 9.6037\text{ \AA}$ ,  $b = 13.3088\text{ \AA}$ ,  $c = 6.4722\text{ \AA}$  with  $\alpha = \beta = \gamma = 90^{\circ}$ . It crystallizes in orthorhombic system with the non-centrosymmetric space group of  $\text{Pca}2_1$ . The Rietveld analysis was performed on the observed PXRD pattern and it was given in figure 2(b). It is worth to mention here that there is no additional peaks were observed which shows the purity of the title compound.

### 3.2. UV-visible spectroscopy

The optical transparency and cutoff wavelength are the important parameters for a nonlinear optical material and it is the key factor for making of optical devices. In the current experimental study, optical transmittance spectra of grown ingot were recorded at room temperature with the wavelength ranging between  $200\text{ nm}$  to  $1100\text{ nm}$ . The transmittance spectrum of the grown crystal is shown in figure 3. The cutoff wavelength was observed to be  $300\text{ nm}$  with an appreciable transmittance in the entire visible region. The lack of absorption in the entire visible region, with lower cutoff wavelength is desirable for effective optical applications [16].



The optical absorption coefficient ( $\alpha$ ) with photon energy ( $h\nu$ ) plays an effective role in the determination of band structure and type of transition of the electron inside the material. The optical absorption coefficient  $\alpha$  can be estimated using the following equation:-

$$\alpha = \frac{2.3026}{t} \log\left(\frac{1}{T}\right) \quad (2)$$

where T is the transmittance and t is the thickness of the specimen which is used for the present measurement.

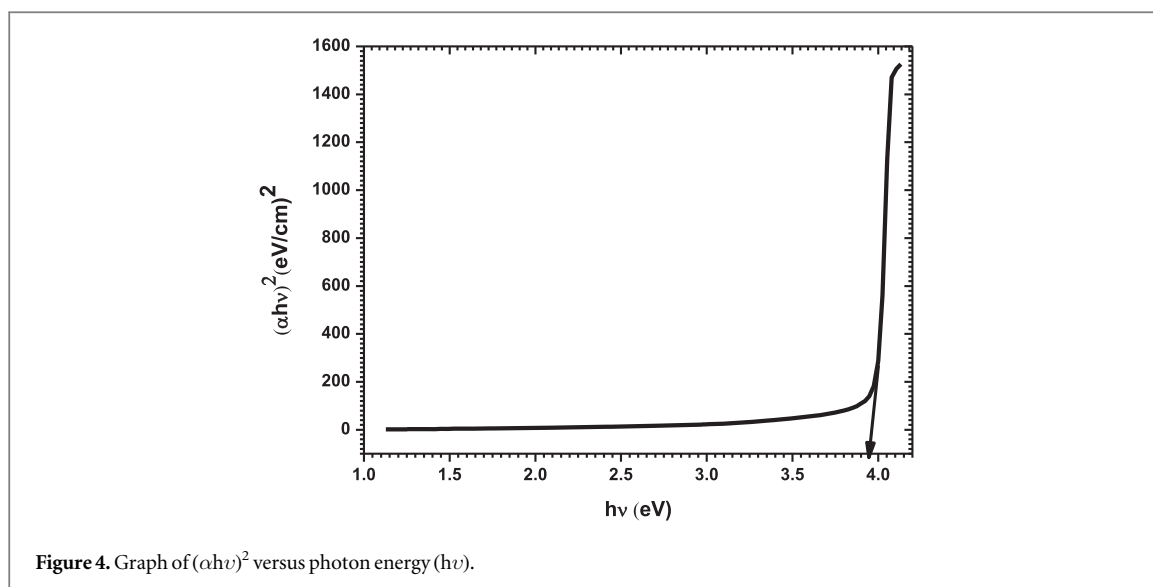


Figure 4. Graph of  $(\alpha h\nu)^2$  versus photon energy ( $h\nu$ ).

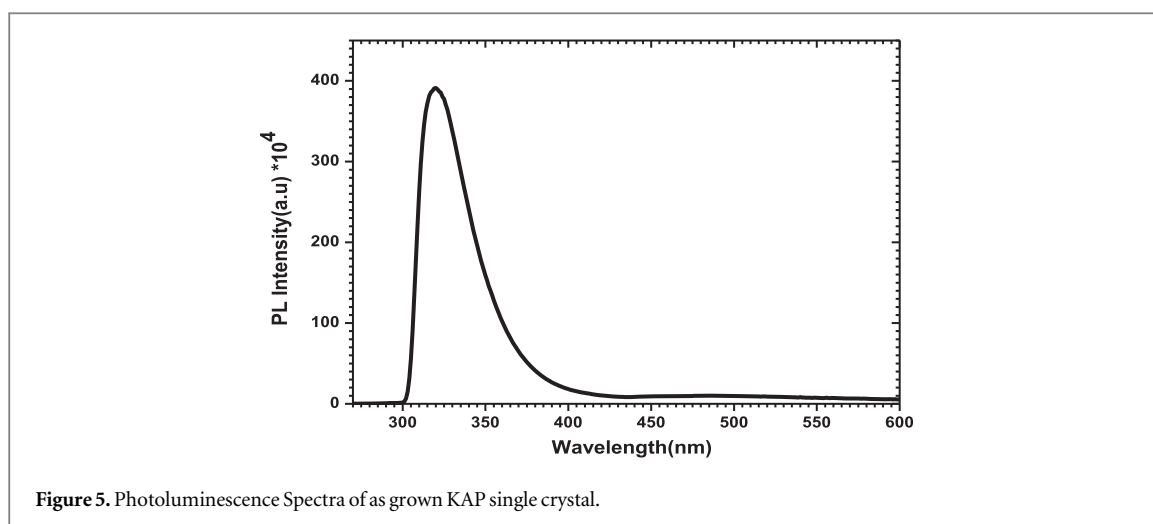


Figure 5. Photoluminescence Spectra of as grown KAP single crystal.

The relation between absorption coefficient ( $\alpha$ ), ( $h\nu$ ) and direct optical band gap ( $E_g$ ) of the incident photon is given in the following equation [17],

$$(\alpha h\nu)^2 = B(E_g - h\nu) \quad (3)$$

where  $E_g$  is the optical band gap of the crystal, B is a constant. The band gap of KAP crystal was calculated from graph  $(\alpha h\nu)^2$  versus  $h\nu$  as displayed in figure 4 and it was found that 3.9 eV. The wide band gap of the crystals confirms the higher transparency in the entire visible region.

### 3.3. Photoluminescence analyses

The photoluminescence (PL) deals with excitation of solid electronic states by certain wavelength or energy which released in term of photons with different wavelengths. The PL emission intensity depends on crystalline nature and the presence of defects in the single crystalline material. In the present study, the photoluminescence measurements were performed using Edinburg instruments (FLS-980, D2D2) and the KAP crystal was excited with a Xenon (Xe) flash lamp at 4.96 eV (250 nm) at room temperature to know about its luminescent behavior of the compound. The spectrum was recorded in the range of 270 nm to 600 nm which is given in figure 5. In the above plot higher intensity peak was observed at 325 nm and one can understand that single crystalline nature of the material. The observed band gap energy is 3.815 eV, which is in tune with the band gap which was calculated from UV-vis., measurements.

In addition to that we have also analyzed the title compound with time resolved PL spectroscopy. In this method, a short pulse is used to excite the material and emission intensity as a function of time is measured with a fast detector. It is a non-destructive technique can be used to know quality of material as exciton life time varies with crystal nature and its defects concentration. The decay time of a particular transition strongly affects the

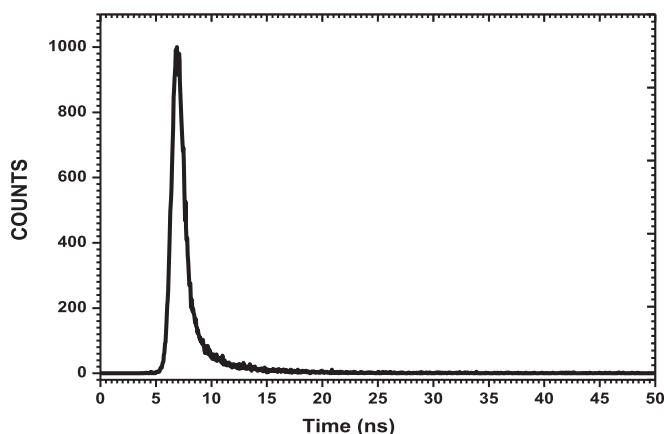


Figure 6. Time Resolved PL decay of KAP recorded at room temperature.

Table 1. Parameters value for time resolved PL.

Parameters	Value
$\tau_1$	0.85 ns
$\tau_2$	4.6 ns
$B_1$	1049.260
$B_2$	50.712
$A_1$	0.314

efficiency of radiative recombination [18]. The decay of PL emission has been recorded at nanosecond scale at room temperature as shown in figure 6 which generally having multi-exponential process with a series of short and long decay components. But in the present study, the decay curve found to follow bi-exponential behavior which can be expressed as,

$$R(t) = A_1 + B_1 \exp(-t/\tau_1) + B_2 \exp(-t/\tau_2) \quad (4)$$

where  $A_1$  is constant with  $\tau_1$  and  $\tau_2$  as the slow and fast components of decay time with constant amplitudes  $B_1$  and  $B_2$  which determine the contribution of slow and fast decay component respectively in all over decay process. The decay profile of PL intensity for KAP single crystal was recorded in a range of 0–50 ns on time scale and spectrum is shown in figure 6. The decay profile is bi-exponentially fitted and the corresponding fitted parameters are shown in the table 1. From this measurement we can understand that it took very short time to come to ground state from excited state. Moreover the relative contribution of slow decay was found to be higher in comparison to the fast decay which can be seen using amplitude value of corresponding decays.

### 3.4. High resolution X-ray diffraction

The quality of KAP single crystal was assessed by using PANalytical X'Pert PRO MRD high-resolution X-ray diffractometer, with  $\text{CuK}\alpha 1$  radiation and information of defects. By using this technique, one can understand the degree of crystallinity in terms of structural grain boundaries; dislocation and nature of defects exist in the grown ingot by recording the diffraction curve (DC). A four-bounce Ge (220) monochromator with a high resolving power was used to generate the highly monochromatic beam with a well defined wavelength and equatorial divergence. To expose the (010) plane, a well polished crystal was loaded to diffractometer and an omega ( $\omega$ ) scan with double axis geometry was performed in symmetrical Bragg geometry. The recorded DC curve is shown in figure 7. The single sharp peak in the DC curve indicates the absence of structural grain boundaries. The full width at half maximum (FWHM) was observed to be  $23''$  which is slightly higher in comparison than that of the theoretical estimation of the diffraction curve by plane wave theory of dynamical X-ray diffraction [19]. The interesting part of the DC is that there is an asymmetry, i.e. the scattered intensity is more in negative side with respect to positive side which points out that the titled single crystal contains primarily vacancy type defects instead of interstitial defects which may be due to fast growth of single crystal. The lattice around the defect core undergoes tensile stress and the inter planar spacing ( $d$ ) for the planes very close to the vacancy defect increases, which leads to diffuse X-ray scattering at angles in the negative area in respect of the exact Bragg peak position. The above explanation can be understood using Bragg equation  $2d \sin \theta = n\lambda$ , where

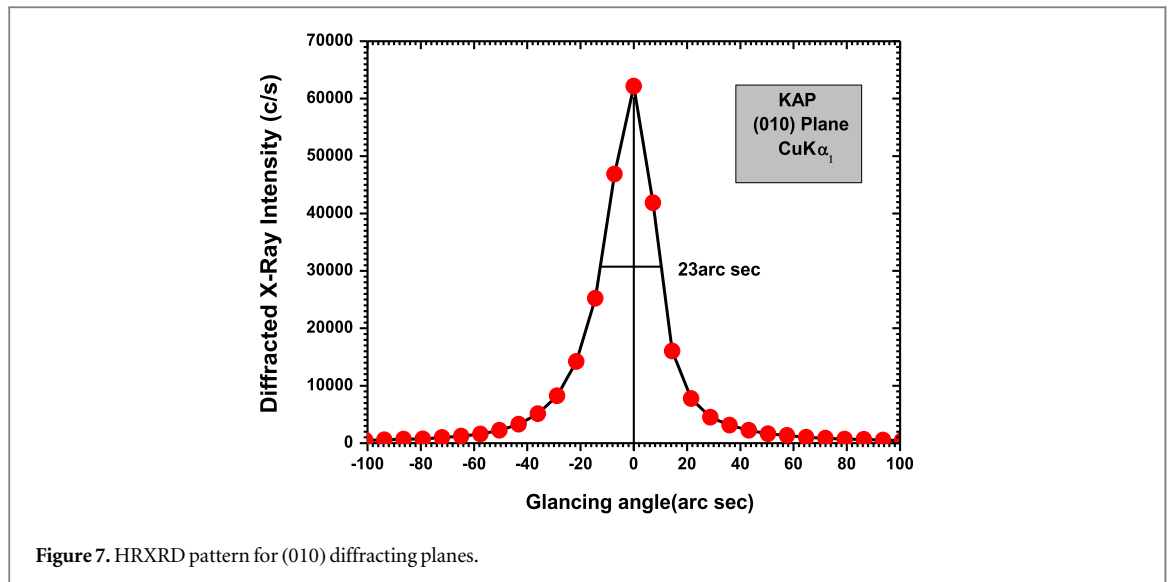


Figure 7. HRXRD pattern for (010) diffracting planes.

$d$  varies inversely with  $\sin \theta$  for fixed value of order of reflection ( $n$ ) and wavelength ( $\lambda$ ). Although the FWHM is moderately low i.e. 23 arc sec, the crystalline perfection is fairly good enough and indicates only a less number of point defects, which can hardly affect the device performance.

### 3.5. Mechanical analysis

Smooth and cleaned transparent single crystal of KAP which is free from cracks and visible inclusions was examined by static indentation tests at ambient temperature. The measurement was performed by using Vickers microhardness tester fixed with a diamond pyramidal shape indenter along with microscope. During the measurement, the dwell time of 10 s was maintained for different loads varying from 5 g to 75 g. Five indentations had been made for each load on the (010) plane of grown crystal and the repeatability of the results were confirmed. Each indentation was obtained and average diagonal length ( $d$ ) was estimated for calculations. A micrometer eyepiece was used to perform all measurements. The Vickers microhardness number  $H_v$  was evaluated using general expression given as:-

$$H_v = 1.8544 \left( \frac{P}{d^2} \right) \quad (5)$$

where applied load ( $P$ ) in Newton and  $d$  in meter and  $H_v$  in Pascal. In addition to that, the above mentioned mechanical analyses can be explained by using the following theoretical models.

#### 3.5.1. Indentation size effect

In general, the value of microhardness will vary with (i) increases with load [20]; (ii) decreases with load [21–25]; (iii) independent of load [26]; (iv) shows complex discrepancy with variation in load [27–29]. In this context, Vickers hardness number versus load for (010) plane is shown in figure 8. We have noticed that the microhardness value decreases with increase of load. This may due to the indenter pierces only upper surface layer of crystal while performing the measurements in lower load region. This leads to substantial decline in hardness value for low load region determined by strain distribution of upper surface layer. The depth penetration of indenter get increase as load increases and both inner and surface layer of the grown crystal contribute to the hardness value. The dominance of inner layers become significant in higher loads and eventually saturation effect is noticed in hardness profile. This shows microhardness deviation with load and can be understood in two regions, one is load dependent and other is load independent. The nature of profile of microhardness variation leads to normal indentation size effect (ISE) and firstly we will explain normal ISE using Meyer's power law,

$$P = Ad^n \quad (6)$$

where  $n$  is the Meyer index and  $A$  is a constant for a given material in a specific crystallographic plane.

A graph of  $\log P$  versus  $\log d$  was plotted and a straight line was obtained which satisfies Mayer's power law as shown in figure 9. The value of ' $n$ ' with material constant  $A$  is given in table 2. Now  $n$  is found to be less than 2 which show normal ISE behavior of microhardness curve. Now combining equations (5) and (6)  $H_v$  can be written in terms of  $d$  as follows:

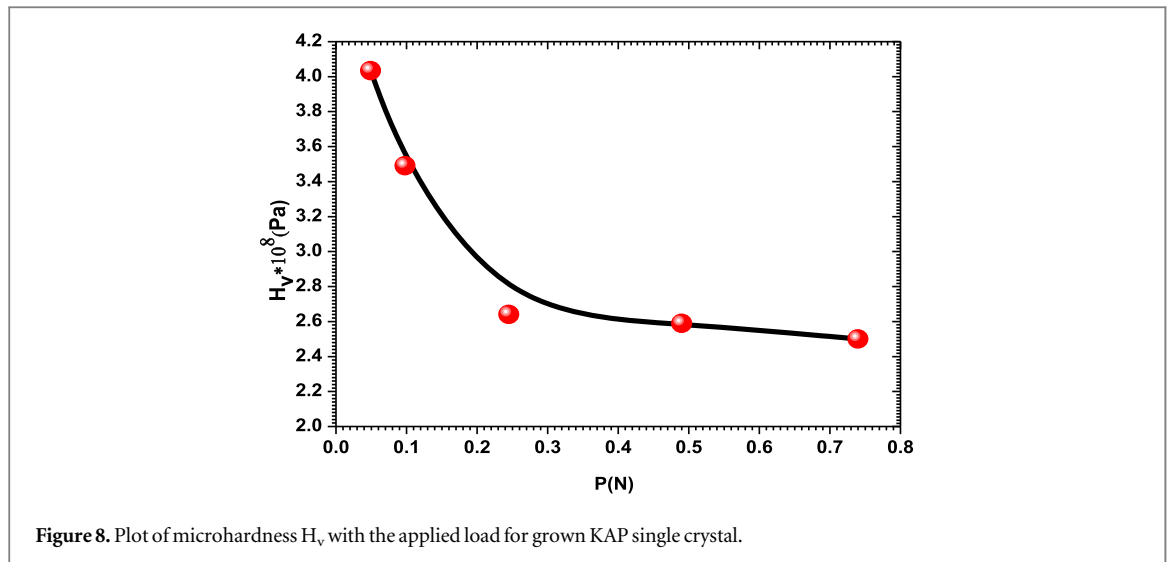


Figure 8. Plot of microhardness  $H_v$  with the applied load for grown KAP single crystal.

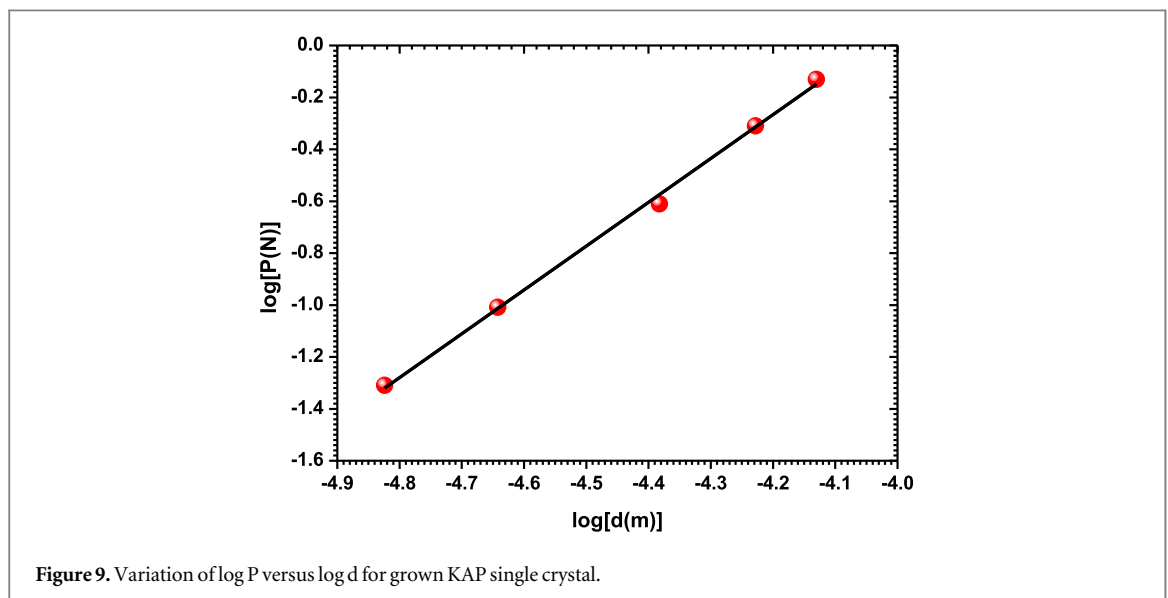


Figure 9. Variation of log P versus log d for grown KAP single crystal.

Table 2. Microhardness parameters for KAP single crystal.

Plane	Mayer's index	Hays and Kendall law and Meyer's law				PSR model	
		A (×10 <sup>7</sup> Pa)	C (×10 <sup>8</sup> Pa)	W (×10 <sup>-2</sup> N)	Slope attained from figure 8(b)	P <sub>c</sub> /d <sub>0</sub> <sup>2</sup> (×10 <sup>8</sup> Pa)	H <sub>0</sub> (×10 <sup>8</sup> Pa)
(010)	1.688	0.6649	1.2647	3.4659	2.3649	1.1282	2.0921

$$H_v = Bd^{n-2} \tag{7}$$

i.e. as  $n < 2$   $H_v$  will decrease with increase of  $d$  and it becomes independent of load as  $n = 2$  which obeys Kick's law [30]. At the same time, it will increase for  $n > 2$ . Moreover in present study the value of  $n > 1.6$  which claims that KAP is a moderately soft crystal category [31].

### 3.5.2. Hays–Kendall's law

The value of microhardness decreases to a certain extent with respect to load, after that which is moving towards higher region. The trend becomes saturated or independent of load which is feasible when  $d$  does not change with  $P$ . This can be easily understood by Hays and Kendall law [32]. This law demonstrates the diagonal length  $d$  is a function of Newtonian resultant pressure ( $P-W$ ) of the specimen. Hays Kendall law can be expressed as:

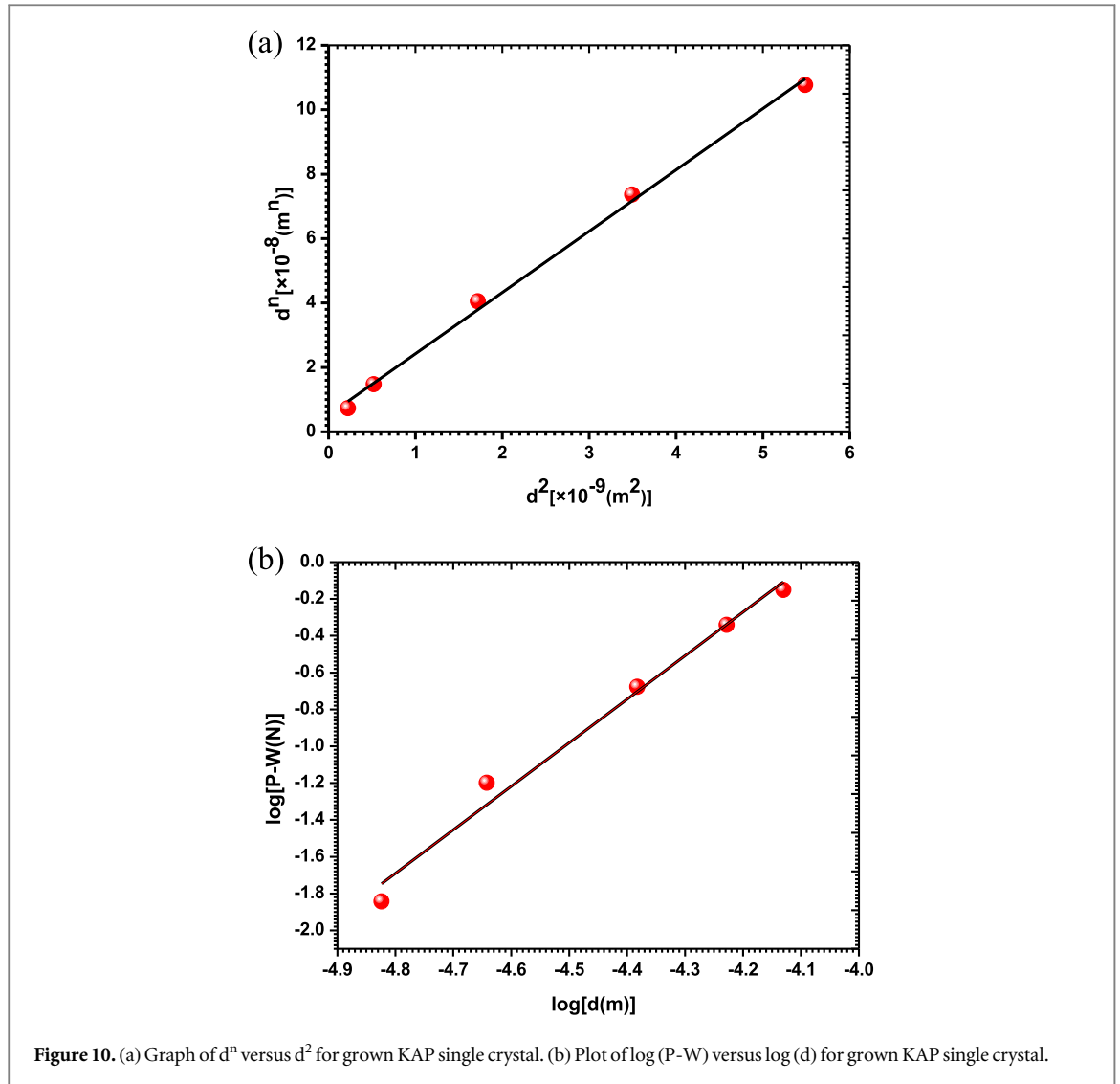


Figure 10. (a) Graph of  $d^n$  versus  $d^2$  for grown KAP single crystal. (b) Plot of  $\log(P-W)$  versus  $\log(d)$  for grown KAP single crystal.

$$P - W = Cd^2 \quad (8)$$

where  $W$  Newtonian resultant pressure and signifies the minimum load that results an indentation i.e. loads less than  $W$  would not allow any plastic deformation,  $C$  is constant and  $n = 2$  is taken as logarithmic index.

Substituting equation (6) for  $P$  in the above expression

$$Ad^n - W = Cd^2 \quad (9)$$

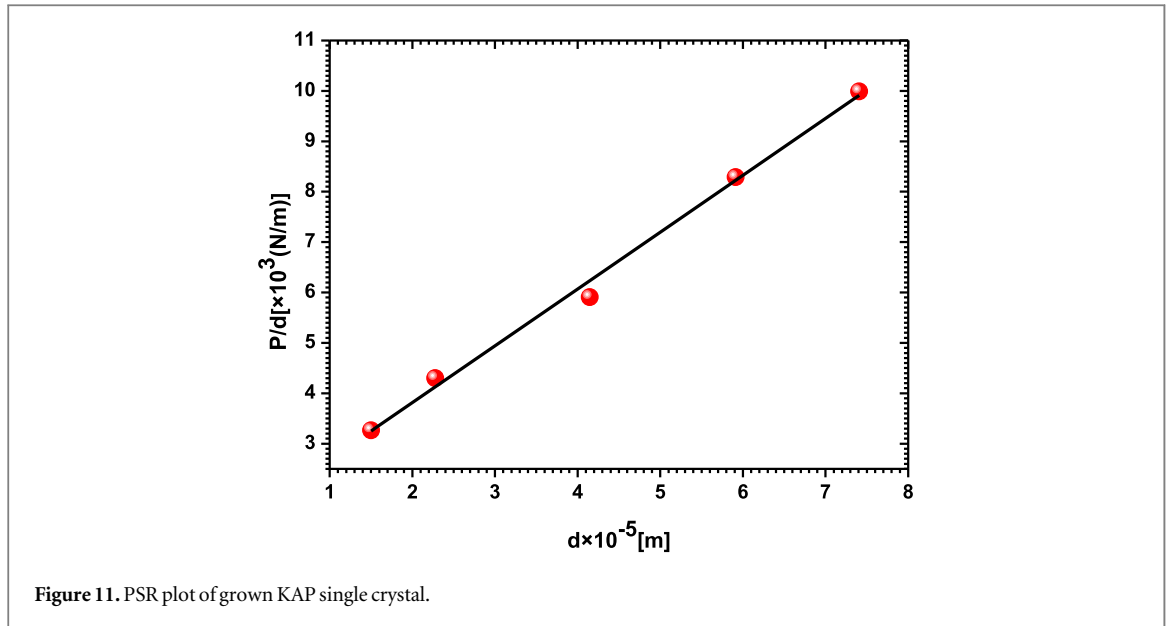
or

$$d^n = \frac{C}{A}d^2 + \frac{W}{A} \quad (10)$$

A plot of  $d^n$  versus  $d^2$  is plotted in figure 10(a) which is a straight line and value of  $C$  and  $W$  was evaluated using the slope  $\left(\frac{C}{A}\right)$  and intercept  $\left(\frac{W}{A}\right)$  as value of  $A$  is already known from the equation (6). The values of constants are shown in table 2. Now after getting the value of  $W$  a graph between  $\log(P-W)$  and the diagonal length  $d$  is plotted as it is shown in figure 10(b). The value of slope is found to be more than 2 which is mentioned in the table 2 disagree the Hays and Kendall law. Moreover value of  $C$  obtained from figures 10(a) and (b) did not match. Hence the mentioned model cannot be employed to know about the behavior of hardness curve of the grown KAP single crystal. Thus, it may be concluded that complete explanation of ISE cannot be understood by simply taking deformation resistance  $W$ .

### 3.5.3. Proportional specimen resistance (PSR) model

The observed hardness value of KAP crystal shows the saturation behavior in the higher loads. Hence, we have tried to calculate the ' $H_0$ ' by using PSR model which was proposed by Li *et al* [33]. According to this model, load  $P$  is related to  $d$  and it is given in the following expression:



$$P = a_1 d + a_2 d^2 \quad (11)$$

where the parameters  $a_1$  is the load dependent microhardness and  $a_2$  is the load independent hardness, which is equal to  $\frac{P_c}{d_0^2}$ . Where  $P_c$  denotes critical load at which saturation of hardness occurs and  $d_0$  is diagonal length. Now equation (11) can be written as,

$$\frac{P}{d} = a_1 + a_2 d \quad (12)$$

A linear variation was found by plotting between  $\frac{P}{d}$  and  $d$  as shown in figure 11 and confirms that the PSR model is applicable for KAP single crystal. The slope of the straight line, when multiplied by the Vickers conversion factor (1.8544) gives the value of the load-independent hardness ' $H_0$ ' which is given in table 2.

### 3.6. Z-scan measurement

The grown crystal of KAP is one of the potential materials for second harmonic generation (SHG) applications and its efficiency is 1.13 times higher than that of standard Potassium Dihydrogen Orthophosphate (KDP) single crystal [34]. In addition to the above said property, it also obeys the third order nonlinear optical behavior which is measured by Z-scan technique which is a simple and famous experimental method for the precise measurements of intensity dependent nonlinear susceptibilities, nonlinear refractive index and the nonlinear absorption (NLA) coefficient and based on the principles of spatial beam distortion [35–38]. It is a single-beam method employed to find out the real and imaginary parts of nonlinear optical susceptibility of a material. The present experiment was performed by standard Z-scan method using a Ti:sapphire (800 nm, 35 fs, 1 KHz repetition rate) laser source. The generated laser pulse was focused using a plano-convex lens of focal length 40 cm with a beam waist of  $\sim 45 \mu\text{m}$ . The well polished KAP crystal of thickness ( $t$ ) 1.62 mm was underwent by this method and the observed variation in transmitted light with Z position was monitored by a detector.

#### 3.6.1. Open Aperture Z-scan technique

In this mode of Z-scan method, aperture in front of detector is absent and detector is sensitive in nonlinear absorption (NLA) case. From the recorded data, one can understand that maximum absorption at focus and this is observed as a valley type which is shown in figure 12. This technique is mainly used when materials exhibits nonlinear absorption such as excited state absorption (ESA), two photon absorption (TPA), saturable absorption (SA) etc. The value of  $\beta$  was evaluated using open aperture Z-scan experimental data using open aperture formula which is represented as follows [39, 40] :-

For  $q_0 < 1$

$$T(z) = \sum_{m=0}^{\infty} \frac{(-q_0)^m}{(m+1)^{3/2}} \quad (13)$$

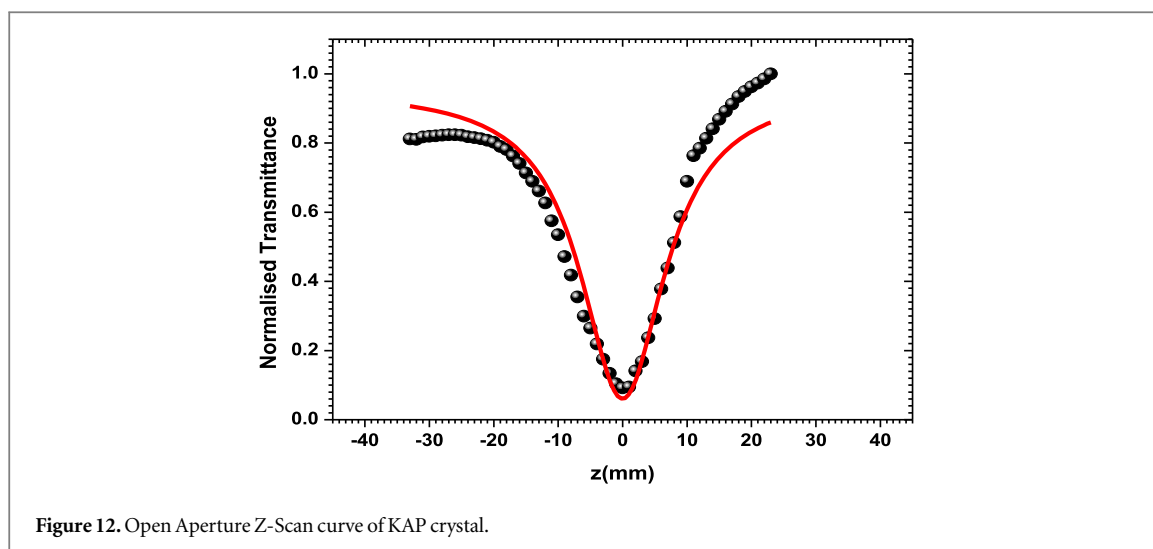


Figure 12. Open Aperture Z-Scan curve of KAP crystal.

By expanding equation (13)  $\alpha_0 \ll 1$

$$T(z) = 1 - \frac{(I_0 L_{\text{eff}} \beta)}{\left[ 2^{\frac{3}{2}} \left( 1 + \frac{z^2}{z_0^2} \right) \right]} \quad (14)$$

Where  $q_0(z)$  depend on parameters  $I_0$ ,  $L_{\text{eff}}$  and  $\beta$  as such

$$q_0 = \frac{I_0 L_{\text{eff}} \beta}{\left( 1 + \frac{z^2}{z_0^2} \right)} \quad (15)$$

where  $L_{\text{eff}}$  is the effective thickness of the sample which can be estimated using  $L_{\text{eff}} = (1 - \exp(-\alpha_0 L)) / \alpha_0$ , where  $L$  is actual thickness of specimen,  $\alpha_0$  is the linear absorption coefficient,  $z$  is specimen position, ( $z_0 = \pi \omega_0^2 / \lambda$ ) is the Rayleigh range and  $I_0$  represents incident intensity of laser beam at focus.

A solid line in figure 12 represents the theoretically calculated and points are the experimentally observed data. The significant value of  $\beta$  at  $I_0 = 2.2 \times 10^{10} \text{ W cm}^{-2}$  for the title compound which can be estimated using experimental data of open aperture of Z-scan,

$$\beta = \frac{2\sqrt{2} \Delta T}{I_0 L_{\text{eff}}} \quad (16)$$

where  $\Delta T$  is  $(1 - T_v)$  where  $T_v$  value of valley in open aperture curve.)

The value of  $\beta$  for grown crystal was found to be  $9.6 \times 10^{-10} \text{ cm W}^{-1}$ . The observed  $\beta$  value conforms that the title compound may be appropriate for optical limiting applications.

## 4. Conclusions

The bulk, defect free and good quality single crystal of KAP was successfully grown by SEST and the grown ingot was thoroughly examined by various characterization techniques. The phase identification, crystal system and lattice parameter was estimated by PXRD using Rietveld analysis. The prominent peaks of observed pattern have been indexed and no extra peak signifies the purity of the material. The transparency and optical band gap studies of the titled single crystal was examined by using UV-vis. spectroscopy. The lower cutoff wavelength and higher transparency range over a long wavelength signify that grown crystal is suitable for optical applications. The HRXRD and PL analyses reveal that the harvested single crystal has minimum defects and may be useful for various applications. Its mechanical behavior was well explained by Vickers microhardness with different theoretical models. Its third order nonlinear optical properties was assessed by Z scan approach and understood that it can be one of the potential materials for nonlinear optical applications.

## Acknowledgments

The authors are thankful to Director, CSIR- NPL for his continuous encouragement in carrying out the present study. The authors are also thankful to Dr G Bhagavannarayana, Dr GA Basheed for useful discussions. One of

the authors Ms Manju Kumari is thankful to CSIR for giving financial assistance through CSIR-Junior Research fellowship (JRF) AcSIR-NPL for PhD registration.

## ORCID iDs

N Vijayan  <https://orcid.org/0000-0003-1552-7676>

Govind Gupta  <https://orcid.org/0000-0001-5006-7623>

## References

- [1] Nalwa H S and Miyata S 1996 *Nonlinear Optics of Organic Molecules and Polymers* (New York, United States of America: CRC Press)
- [2] Prasad P N and Williams D J 1991 *Introduction to Nonlinear Optical Effects in Molecules and Polymers* (New York: Wiley)
- [3] Jones J L, Paschen K W and Nicholson J B 1963 *J. Appl. Opt.* **2** 955–61
- [4] Yoda O, Miyashita A, Murakami K, Aoki S and Yamaguchi N 1991 *Proc. SPIE Int. Soc. Opt. Eng.* **1503** 463–6
- [5] Nisoli M, Pruneri V, Magni V, De Silvestri S, Dellepiane G, Comoretto D, Cuniberti C and Le Moigne J 1994 *Appl. Phys. Lett.* **65** 590–2
- [6] Timpanaro S, Sassella A, Borghesi A, Porzio W, Fontaine P and Goldmann M 2001 *Adv. Mater.* **13** 127–30
- [7] Miniewicz A and Bartkiewicz S 1993 *Adv. Mat. Opt. Elect.* **2** 157–63
- [8] Ester G R and Halfpenny P J 1998 *J. Cryst. Growth* **187** 111–8
- [9] Hottenhuis M H J and Lucasius C B 1986 *J. Cryst. Growth* **78** 379–88
- [10] Okaya Y 1965 *Acta Cryst.* **19** 879–82
- [11] Alex A V and Philip J 2000 *J. Appl. Phys.* **88** 2349–51
- [12] Bore J and Sangwal K 2004 *Surf. Sci.* **555** 1–10
- [13] Kejalakshmy N and Srinivasan K 2003 *J. Phys. D Appl. Phys.* **36** 1778
- [14] Srinivasan K, Meera K and Ramasamy P 1999 *J. Cryst. Growth* **205** 457–9
- [15] Enculescu M 2010 *Physica. B* **405** 3722–7
- [16] Levanyuk A P, Osipov V V, Sigov A S and Sobyenin A A 1979 *J. Exp. Theor. Phys.* **76** 345–68
- [17] Ashour A, El-Kadry N and Mahmoud S A 1995 *Thin Solid Films* **269** 117–20
- [18] Vijayan N, Philip J, Haranath D, Rathi B, Bhagavannarayana G, Halder S K, Roy N, Jayalakshmy M S and Verma S 2014 *Spectrochim. Acta A Mol. Biomol. Spectrosc.* **122** 309–14
- [19] Batterman B W and Cole H 1964 *Rev. Mod. Phys.* **36** 681–717
- [20] Vengatesan B, Kanniah N and Ramasamy P 1986 *J. Mater. Sci. Lett.* **5** 987–8
- [21] Kotru P N, Razdan A K and Wanklyn B M 1989 *J. Mater. Sci.* **24** 793–803
- [22] Pratap K J and Babu V H 1980 *Bull. Mater. Sci.* **2** 43–53
- [23] Bamzai K, Kotru P N and Wanklyn B M 1996 *Cryst. Res. Technol.* **31** 813–9
- [24] Balakrishnan K, Vengatesan B, Kanniah N and Ramasamy P J. *Mater. Sci. Lett.* **9** 785–7
- [25] Tickoo R, Tandon R P, Bamzai K K and Kotru P N 2003 *Mater. Chem. Phys.* **80** 446–51
- [26] Ascheron C, Haase C, Kühn G and Neumann H 1989 *Cryst. Res. Technol.* **24** K33–5
- [27] Bhatt V P, Patel R M and Desai C F 1983 *Cryst. Res. Technol.* **18** 1173–9
- [28] Dhar P R, Bamzai K and Kotru P N 1997 *Cryst. Res. Technol.* **32** 537–44
- [29] Guille J and Sieskind M 1991 *J. Mater. Sci.* **26** 899–903
- [30] Mott B W 1956 *Microindentation Hardness Testing* (London: Butterworths)
- [31] Onitsch E M 1947 *Mikroskopie* **2** 131–51
- [32] Hays C and Kendall E G 1973 *Metallography* **6** 275–82
- [33] Li H and Bradt R C 1991 *Mater. Sci. Eng. A* **142** 51–61
- [34] Viji Niraimathi D and Shanthi C 2015 *J. Chem. Crystallogr.* **45** 376–82
- [35] Choubey R K, Medhekar S, Kumar R, Mukherjee S and Kumar S 2014 *J Mater Sci: Mater Electron* **25** 1410–5
- [36] Dadhich B K, Kumar I, Choubey R K, Bhushan B and Priyam A 2017 *Photochem. Photobiol. Sci.* **16** 1556–62
- [37] Medhekar S, Kumar R, Mukherjee S and Choubey R K 2013 *AIP Conf. Proc.* **1512** 470–1
- [38] Choubey R K, Trivedi R, Das M, Sen P K, Sen P, Kar S, Bartwal K S and Ganeev R A 2009 *J. Cryst. Growth* **311** 2597–601
- [39] Sheik-Bahae M, Said A A and Van Stryland E W 1989 *Opt. Lett.* **14** 955–7
- [40] Sheik-Bahae M, Said A A, Wei T-H, Hagan D J and Van Stryland E W 1990 *IEEE J. Quantum Electron.* **26** 760–9